# STRUCTURE OF POTASSIUM GERMANATE GLASSES BY VIBRATIONAL SPECTROSCOPY

Y.D. YIANNOPOULOS[a], E.I. KAMITSOS[a] and H. JAIN[b]
[a]Theoretical and Physical Chemistry Institute,
National Hellenic Research Foundation,
48 Vass. Constantinou Ave., Athens 116 35, Greece

[b]Department of Materials Science and Engineering,
Lehigh University, Bethleehem, PA 18015, USA

## 1. Introduction

The use of germanate glasses in technological applications, such as optical fibers and infrared transmitting windows, has stimulated extensive investigations of their physical properties. The refractive index, density, thermal expansion coefficient, and electrical conductivity of alkali germanates were found to exhibit extrema as a function of alkali oxide content [1-4]. This behaviour is widely known as the "germanate anomaly effect".

To explain this anomalous behaviour, it was proposed that addition of alkali oxide ($M_2O$) to $GeO_2$ causes the partial conversion of germanium-oxygen tetrahedra into octahedral units when the alkali content is up to 20-25 mol% $M_2O$, while higher $M_2O$ concentrations cause the formation of non-bridging oxygen (NBO) containing germanate tetrahedra [5-12]. In a different approach, it was proposed that the formation of non-bridging oxygens is the only modification mechanism of the germanate network [13].

In this work, infrared reflectance and Raman spectroscopies are employed in an attempt to investigate the structural origin of the germanate anomaly effect in the $xK_2O.(1-x)GeO_2$ glass system. In particular, emphasis is placed on understanding the compositional dependence of germanium coordination and the bonding state of oxygen atoms.

## 2. Experimental

Glass samples in the system $xK_2O.(1-x)GeO_2$ were prepared by melting in Pt crucibles stoichiometric amounts of polycrystalline $GeO_2$ and $K_2CO_3$ at ~1150°C for *ca* 0.5-2



*A. Andriesh and M. Bertolotti (eds.),*
*Physics and Applications of Non-Crystalline Semiconductors in Optoelectronics*, 317–325.

hrs depending on composition. Splat-quenching the melt resulted in glasses with $K_2O$ contents in the range $0 \leq x \leq 0.55$.

Raman spectra were measured using a Ramanor HG 2S Jobin-Yvon spectrometer and the 488nm line of a Spectra Physics argon ion laser for excitation. The glass sample was placed in a vacuum cell to eliminate hydrolysis effects.

Infrared spectra were recorded in the specular reflectance mode on a vacuum spectrometer (Bruker 113v). The reflectance data in the range 20-4000 $cm^{-1}$ were analysed by the Kramers-Krönig inversion technique. The reported here absorption coefficient spectra $\alpha(\nu)$, were calculated by the expression $\alpha(\nu)=4\pi\nu k(\nu)$, where $k(\nu)$ is the imaginary part of the refractive index and $\nu$ is the frequency in $cm^{-1}$ [14].

## 3. Results and Discussion

### 3.1. RAMAN SPECTRA

Raman spectra of $xK_2O.(1-x)GeO_2$ glasses are shown in Figures 1 and 2 in the ranges $0 \leq x \leq 0.20$ and $0.24 \leq x \leq 0.55$, respectively. These spectra show considerable agreement with spectra published earlier by Verweij and Buster [8] and Furukawa and White [9].

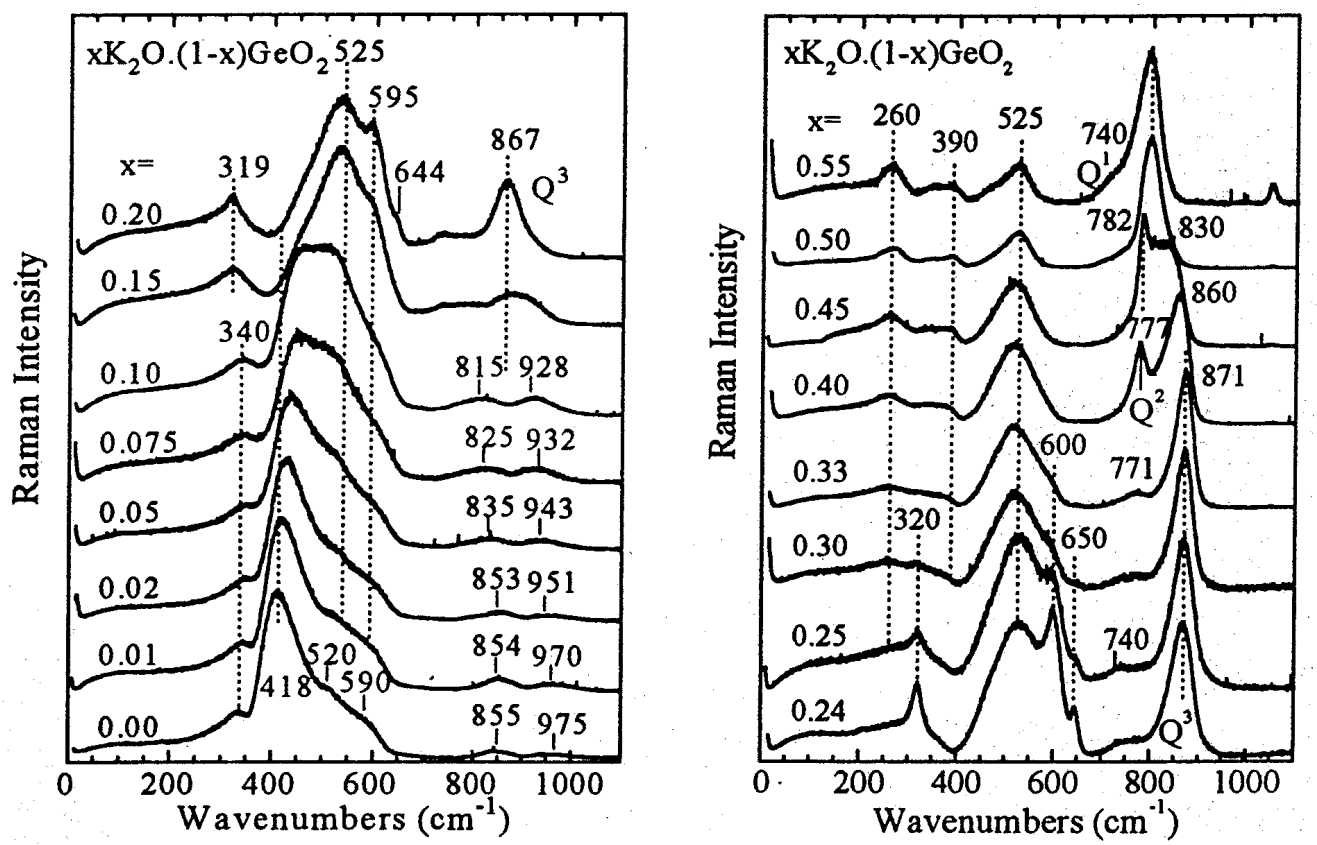


*Figure 1.* (left) Raman spectra of $xK_2O.(1-x)GeO_2$ glasses ($0 \leq x \leq 0.20$).
*Figure 2.* (right) Raman spectra of $xK_2O.(1-x)GeO_2$ glasses ($0.24 \leq x \leq 0.55$).

The dominant feature of the $GeO_2$ glass (x=0) at 418 $cm^{-1}$ is attributed to the symmetric stretching vibration of Ge(4)-O-Ge(4) bridges ($\nu_s$ (Ge(4)-O-Ge(4)) in six-membered rings, i.e. rings containing six $GeO_4$ tetrahedra [15,16]. The number in parenthesis indicates the coordination number of Ge atoms. Upon increasing $K_2O$ content this band decreases in intensity and eventually vanishes at $x \cong 0.25$ indicating the distruction of such tetrahedra containing ring arrangements.

Three bands at *ca* 320, 600 and 650 $cm^{-1}$ develop with increasing x, attain their maximum relative intensity at $x \cong 0.24$ and then diminish for $x > 0.40$. Previous Raman studies of glassy and crystalline alkali germanates have demonstrated that the presence of these bands is related to the formation of interconnected $GeO_6^{-2}$ octahedral units [14,17,18]. Specifically, bands in the range 550-650 $cm^{-1}$ were attributed to $\nu_s$ (Ge(6)-O-Ge(6)) [14]. Besides these features, a new band develops at *ca* 525 $cm^{-1}$ with increasing x. As shown elsewhere [14] this band can been assigned to $\nu_s$ (Ge(4)-O-Ge(6)), i.e. to bridges connecting a germanium tetrahedron with a germanium octahedron, without excluding some contribution from $\nu_s$ (Ge(4)-O-Ge(4)) in three-membered rings of $GeO_4$ tetrahedra.

For $x \geq 0.10$ a new band develops at 867 $cm^{-1}$ and becomes the dominant Raman feature for x=0.33. This band is assigned to the symmetric stretching vibration of Ge-$O^-$ bonds ($O^-$=NBO) in germanate tetrahedra containing three bridging and one non-bridging oxygen [14]. This is the so called $Q^3$ unit, where the notation $Q^n$ indicates a germanium tetrahedron with 4-n non-bridging oxygens per Ge atom. Thus a new type of bridge, Ge(4)-O-Ge($Q^3$), is formed with one Ge atom being of $Q^3$ type. It is expected that the symmetric stretching vibration of the new bridges, $\nu_s$ (Ge(4)-O-Ge($Q^3$)), will also contribute to the 510-530 $cm^{-1}$ range.

Increasing further the $K_2O$ content ($x > 0.30$) causes additional modifications to the germanate structure as evidenced by the appearance of the new band at 770-780 $cm^{-1}$ and the shoulder at *ca* 740 $cm^{-1}$ ($x > 0.50$). The new features are attributed to the symmetric stretching vibration of Ge-$O^-$ bonds in $Q^2$ and $Q^1$ germanate tetrahedra respectively [8,9,14]. Therefore, high alkali oxide contents lead to the progressive depolymerization of the germanate network through formation of non-bridging oxygen atoms.

In an attempt to semiquantify the effect of $K_2O$ on the relative abundance of the various structural units composing the germanate network, we have deconvoluted the complex profile from 350-650 $cm^{-1}$. A typical example of deconvolution is shown in the inset of Fig. 3 for the x=0.20 glass. The three spectral ranges considered are: 418-450 $cm^{-1}$ (A), characteristic of Ge(4)-O-Ge(4) bridges mostly in six-membered rings; 515-530 $cm^{-1}$ (B) resulting from Ge(4)-O-Ge(4) bridges in three-membered rings and mixed bridges such as Ge(4)-O-Ge(6) and bridges where at least one Ge atom contains NBO's, e.g. Ge(4)-O-Ge($Q^3$) and Ge($Q^3$)-O-Ge($Q^2$); and 600 $cm^{-1}$+650 $cm^{-1}$ (C) characteristic of *connected* $GeO_6$ octahedra. The composition dependence of the relative intensity of these selected Raman bands (Fig. 3) show clearly that the relative abundance of $GeO_4$ tetrahedra in six-membered rings decreases monotonically with x and vanishes for $x \cong 0.40$ (curve A), while the relative population of *connected* $GeO_6$ octahedra attains its maximum value at ~24mol% $K_2O$ (curve C). This indicates

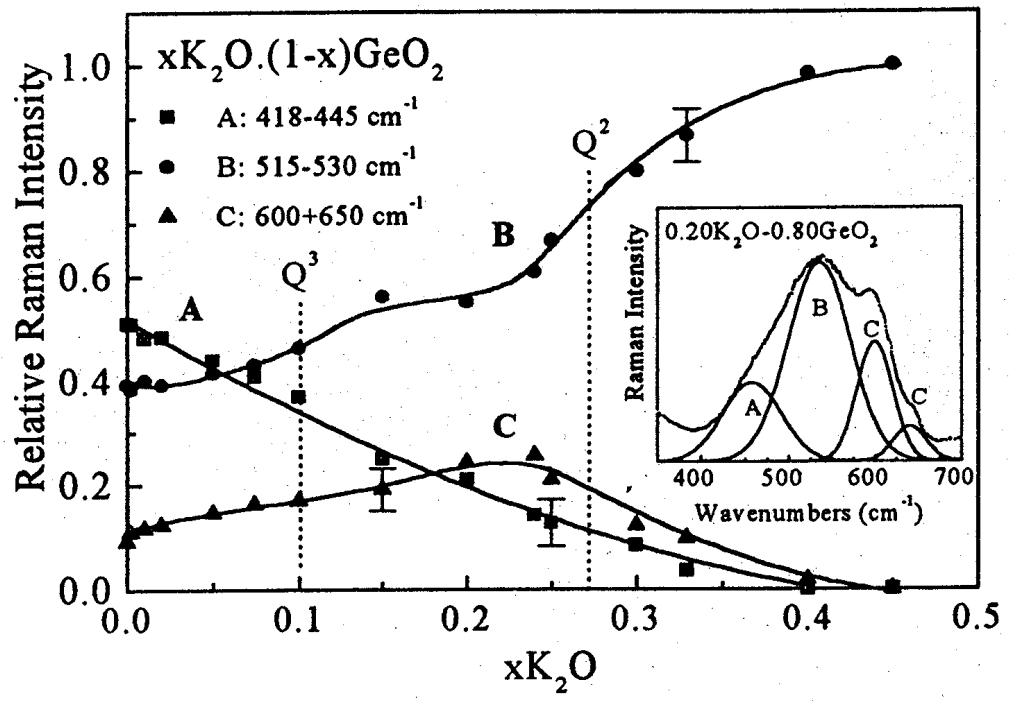


*Figure 3.* Composition dependence of the relative intensity of deconvoluted bands in the 350-700 $cm^{-1}$ Raman envelope of $xK_2O.(1-x)GeO_2$ glasses. Lines are drawn to guide the eye. The vertical dotted lines indicate the approximate onset for formation of $Q^3$ and $Q^2$ germanate tetrahedra. The inset shows an example of deconvolution (x=0.20).

that the $GeO_4 \rightarrow GeO_6$ conversion is the dominant modification mechanism up to $x \approx 0.25$, in agreement with the recent studies of K-germanates by XPS and EXAFS [19,20]. The composition dependence of curve B (515-530 $cm^{-1}$) is more complicated because of the combined contribution of at least four different bridges as discussed above. A more detailed discussion of the Raman spectra will be presented in a future publication.

## 3.2 INFRARED SPECTRA

### *3.2.1 Spectral Assignments*

The infrared absorption spectra of $xK_2O.(1-x)GeO_2$ glasses are presented in Figures 4 and 5 for $0 \leq x \leq 0.45$. Clearly, addition of $K_2O$ to $GeO_2$ causes progressive spectral changes in the entire infrared range. However, for the purpose of this work we consider only the high frequency envelope (600-1100 $cm^{-1}$). For $x \leq 0.20$ a monotonic downshift of the high-frequency envelope is observed, while for higher modification levels it splits initially into two components ($0.20 \leq x \leq 0.33$) and then develops into a broad band ($x \geq 0.40$) with a shoulder at *ca* 650 $cm^{-1}$. The intense band of $GeO_2$ at 915 $cm^{-1}$ is assigned to the asymmetric stretching vibration of Ge(4)-O-Ge(4) bridges; designated by $\nu_{as}$ (Ge(4)-O-Ge(4)) [14-16]. The asymmetry of this band reveals a broad distribution of intertetrahedral Ge-O-Ge angles. For low $K_2O$ contents ($x<0.02$), the

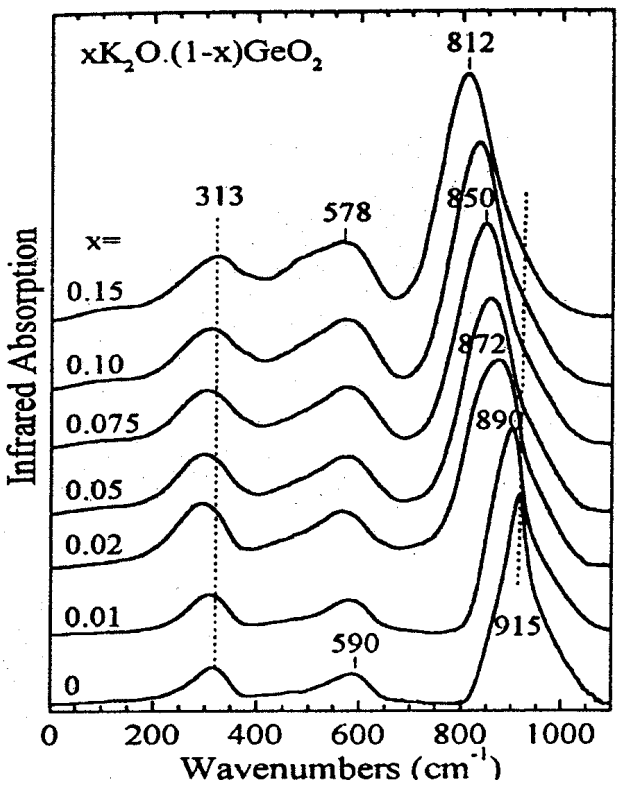


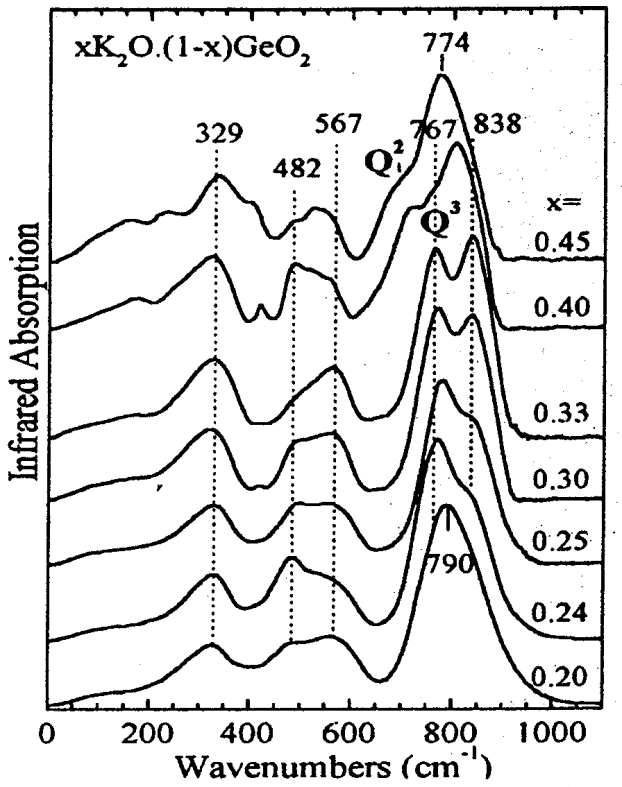


*Figure 4 (left).* IR spectra of $xK_2O.(1-x)GeO_2$ glasses ($0 \leq x \leq 0.15$).
*Figure 5 (right).* IR spectra of $xK_2O.(1-x)GeO_2$ glasses ($0.20 \leq x \leq 0.45$).

rapid decrease of $\nu_{as}$ (Ge(4)-O-Ge(4)) can be explained in terms of the change in rings statistics in favour of the smaller three membered rings. As shown in the case of rubidium germanate glasses, a decrease of the average Ge(4)-O-Ge(4) angle by ~5° can cause a lowering of $\nu_{as}$ (Ge(4)-O-Ge(4)) by as much as 25 $cm^{-1}$ [14].

For higher $K_2O$ contents, the $GeO_4 \rightarrow GeO_6$ transformation mechanism, as well as the formation of NBO containing units take place as shown from the consideration of the Raman spectra. Therefore, the complexity of the induced structural changes makes deconvolution of the 650-1100 $cm^{-1}$ envelope necessary. Typical examples of deconvoluted infrared profiles are shown in Figure 6. For $x>0.01$, the gradual destruction of Ge(4)-O-Ge(4) bridges (intensity decrease of the band centered at ~890 $cm^{-1}$) is followed by the creation of new types of bridges and therefore the development of new bands. Thus, the formation of octahedral units gives rise to the band at ~850 $cm^{-1}$ ($\nu_{as}$ (Ge(4)-O-Ge(6))), and the creation of $Q^3$ species to the band in the range ~800-770 $cm^{-1}$ ($\nu_{as}$ (Ge-$O^-$) [5,14]). In the recent XPS study of potassium germanate glasses NBO's were detected at $K_2O$ content as low as 2mol% [19]. The relative abundance of $Q^3$ species dominates at x=0.33, in agreement with the Raman spectra presented in Fig. 2. The new feature in the range 820-830 $cm^{-1}$ evolving for $x>0.25$ is attributed to the $\nu_{as}$ (Ge-O-Ge) where at least one of the germanium atoms contains NBO's (i.e. $Q^3$, $Q^2$). The formation of $Q^2$ units for $x>0.25$ is signaled by the band developing at ~700 $cm^{-1}$, $\nu_{as}$ (Ge-$O^-$).

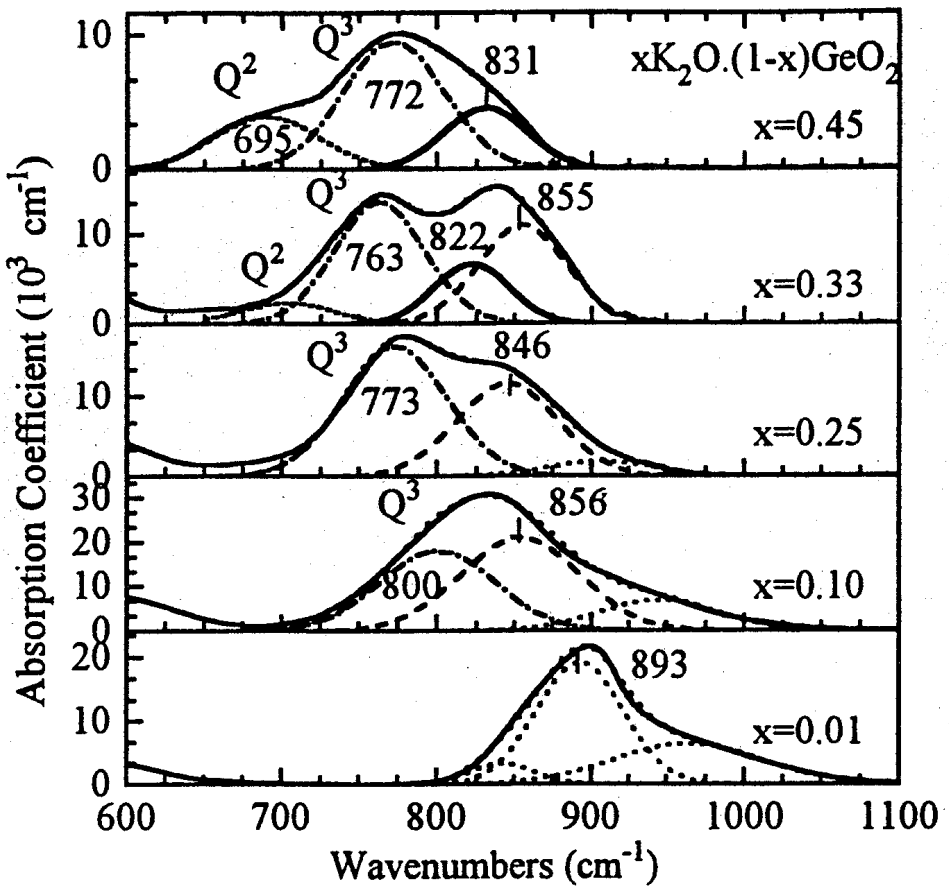


*Figure 6.* Examples of deconvoluted high frequency envelope of the infrared spectra of potassium germanate glasses. For details see text.

*3.2.2 Coordination of Ge atoms in K-germanate glasses*

As shown previously [14], the frequency of the asymmetric stretching of Ge-O-Ge bridges perturbed by the presence of $GeO_6$ octahedral units ($\nu_{as}$ (Ge(4)-O-Ge(6)) can be used to estimate the average coordination number of germanium atoms. The Dachille and Roy [21] semiempirical relation between $\nu_{as}$ and the coordination number (CN) of the glass forming cation takes the following form for the case of germanate glasses:

$$K=5.6CN/\lambda^2$$

where the constant K was estimated to be K=0.172 and the wavelength $\lambda=(\nu_{as})^{-1}$ is given in μm. The results for the composition dependence of CN (Ge), using for the $\nu_{as}$ (Ge(4)-O-Ge(6)) frequencies the values obtained by deconvolution, are shown in Figure 7(a). It is very clear that the CN of Ge atoms changes with $K_2O$ addition to $GeO_2$ and attains its maximum value (CN≅4.32) at ~25mol% $K_2O$. This is in good agreement with previously published results by Sakka and Kamiya [7] (CNmax~4.46) and Huang et al. [20] (CNmax~4.2) employing different spectroscopic techniques.

The fraction of Ge atoms in six-fold coordination was estimated from the relation: $N_6=(CN/2)-2$ and is shown in Figure 7(b) *vs* $xK_2O$. The solid line represents the theoretical curve, $N_6=x/(1-x)$, if no NBO's were formed. $N_6$ values obtained from

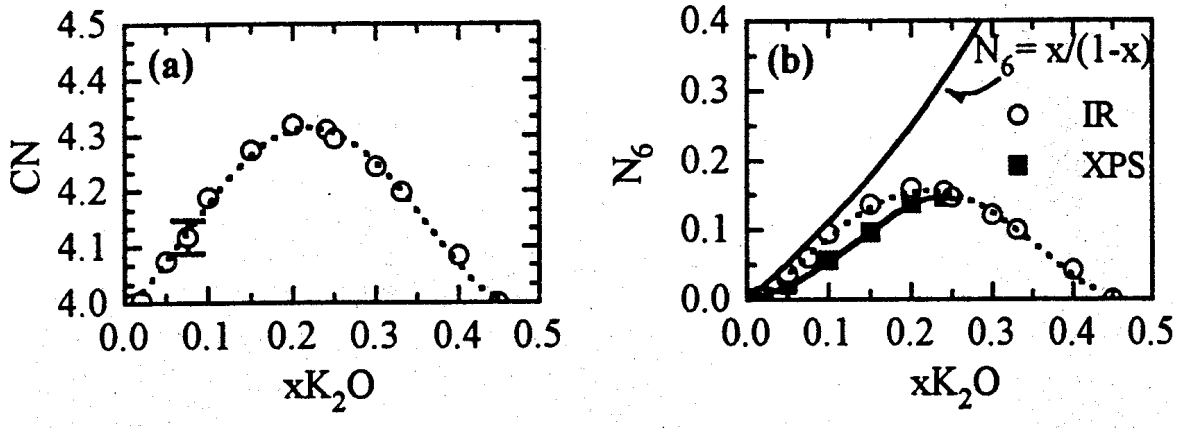


*Figure 7.* Composition dependence of the coordination of Ge atoms, CN (a) and of the fraction of Ge atoms in six-fold coordination, $N_6$ (b) in $xK_2O.(1-x)GeO_2$ glasses. IR and XPS denote $N_6$ values obtained from the analysis of infrared and XPS data respectively.

XPS spectroscopy [19] are also shown for comparison. It is evident that the results from both spectroscopic techniques are in considerable agreement. Deviation of the experimental $N_6$ values from the theoretical curve, mainly for $x>0.25$, indicates the increasing rate of NBO formation.

## 4. Conclusions

Potassium germanate glasses $xK_2O.(1-x)GeO_2$ were prepared over the entire glass forming region, $0\leq x\leq 0.55$, and studied by infrared reflectance and Raman spectroscopies in order to investigate the composition dependence of the structural modification mechanisms.

In glasses with low $K_2O$ content ($0\leq x<0.02$), six-membered rings rearrange to form smaller rings; probably three-membered ones. This process is manifested by the abrupt downshift of the high frequency envelope of the infrared spectra.

For $K_2O$ contents up to $x=0.25$, the $GeO_4 \rightarrow GeO_6$ conversion mechanism dominates. In the Raman spectra this is manifested by the progressive evolution, and then the disappearance of the bands at *ca* 320, 600 and 650 $cm^{-1}$, while the infrared analysis showed that the average coordination number of Ge atoms increases and attains its maximum value (~4.32) at $x\cong 0.25$.

The formation of non-bridging oxygens (NBO's) in various $Q^n$ species is the main structural modification process for $x>0.25$. The progressive depolymerization of the germanate network through NBO formation is followed by the development of high frequency bands in the Raman spectra, due to the localized vibration of the $Ge\text{-}O^-$ bonds, and by the increasing deviation of the experimental $N_6$ values from the theoretical curve.

**Acknowledgments.** This work was supported by NATO Collaborative Research Grants Program (CRG 931213), NHRF, and USDoE.

## 5. References


1. Murthy, K. M. and Aguayo, J. (1964) Studies in germanium oxide systems: II, phase equilibria in the system $Na_2O$-$GeO_2$, *J. of the American Ceramic Society* **47**, 444-447.
2. Shelby, J.E. (1974) Viscosity and thermal expansion of alkali germanate glasses, *J. of the American Ceramic Society* **57**, 436-439.
3. Mundy, J.N. and Jin, G.L. (1987) Ionic transport in rubidium aluminogermanate glasses, *Solid State Ionics* **24**, 263-272.
4. Sakai, T., Nagoya, T., Takizawa, K. and Sekizawa, T. (1995) Electrical conductivity of $K_2O$-$GeO_2$ glasses and germanate anomaly, *Denki Kagaku* **63**, 608-612.
5. Murthy, M.K. and Kirby, E.M. (1964) Infrared spectra of alkali-germanate glasses, *Physics and Chemistry of Glasses* **5**, 144-146.
6. Riebling, E.F. (1972) Infrared study of polymerisation in silver, thallium, and thallium aluminogermanate glasses, *J. of Materials Science* **7**, 40-46.
7. Sakka, S. and Kamiya, K. (1982) Structure of alkali germanate glasses studied by spectroscopic techniques, *J. Non-Crystalline Solids* **49**, 103-116.
8. Verweij, H. and Buster, J.H.J.M. (1979) The structure of lithium, sodium and potassium germanate glasses, studied by Raman scattering, , *J. Non-Crystalline Solids* **34**, 81-99.
9. Furukawa, T. and White, W.B. (1980) Raman spectroscopic investigation of the structure and crystallization of binary alkali germanate glasses, *J. of Materials Science* **15**, 1648-1662.
10. Kamiya,K., Yoko, T., Itoh, Y. and Sakka, S. (1986) X-ray diffraction study of $Na_2O$-$GeO_2$ melts, *J. Non-Crystalline Solids* **79**, 285-294.
11. Cox, A.D. and McMillan, P.W. (1981) An EXAFS study of the structure of lithium germanate glasses, *J. Non-Crystalline Solids* **44**, 257-264.
12. Huang, W.C., Jain, H. and Marcus, M.A. (1994) Structural study of Rb and (Rb,Ag) germanate glasses by EXAFS and XPS *J. Non-Crystalline Solids* **180**, 40-50.
13. Henderson, G.S. and Fleet, M.E. (1991) The structure of glasses along the $Na_2O$-$GeO_2$ join, *J. Non-Crystalline Solids* **134**, 259-269.
14. Kamitsos, E.I., Yiannopoulos, Y.D., Karakassides, M.A., Chryssikos, G.D. and Jain, H. (1996) Raman and Infrared Structural Investigation of $xRb_2O{\cdot}(1-x)GeO_2$ Glasses, *J. Physical Chemistry* **100**, 11755-11765.
15. Galeener, F. L. (1979) Band limits and the vibrational spectra of tetrahedral glasses, *Physical Review B* **19**, 4292-4297.
16. Sharma, Shiv K., Matson, D.W., Philpotts, J.A. and Roush, T.L. (1984) Raman study of the structure of glasses along the join $SiO_2$-$GeO_2$, *J. Non-Crystalline Solids* **68**, 99-114.
17. Mochida, N., Sakai, K. and Kikuchi, K. (1984) Raman spectroscopic study of the structure of the binary alkali germanate glasses, *Yogyo Kyokai Shi*, **92**, 164-172.

18. Durben, D.J. and Wolf, G.H. (1991) Raman spectroscopic study of the pressure-induced coordination change in $GeO_2$ glass, *Physical Review B* **43**, 2355-2363.
19. Lu, X., Jain, H. and Huang, W.C. (1996) Structure of potassium and rubidium germanate glasses by x-ray photoelectron spectroscopy, *Physics and Chemistryof Glasses* **37**,201-205.
20. Huang, W.C., Jain, H. and Meitzner, G. (1996) The structure of potassium germanate glasses by EXAFS, *J. Non-Crystalline Solids* **196**, 155-161.
21. Dachille, F. and Roy, R. (1959) The use of infrared absorption and molar refractivities to check coordination, *Zeitschrift Kristallographie* **111**, 462-470.